Received: 5 December 2017 | Revised: 12 January 2018 | Accepted: 12 January 2018

DOI: 10.1002/aoc.4311

FULL PAPER

WILEY Applied Organometallic Chemistry

Synthesis, cytotoxicity and anti-metastatic properties of new pyridyl–thiazole arene ruthenium(II) complexes

Li Wang | Yihui He | Guangya Xiang | Xianmei Shang

Tongji School of Pharmacy, Huazhong University of Science and Technology, 13 Hangkong Road, Wuhan 430030, People's Republic of China

Correspondence
Xianmei Shang, Tongji School of Pharmacy, Huazhong University of Science and Technology, 13 Hangkong Road, Wuhan 430030, People's Republic of China.
Email: shangxianmei@hust.edu.cn

Funding information
Natural Science Foundation of Hubei Province of China, Grant/Award Number: 2016CFB433; Fundamental Research Funds for the Central Universities of China, Grant/Award Number: 2015TS131; National Natural Science Foundation of China, Grant/Award Number: 81102311

A series of novel ruthenium(II)–cymene complexes (**1**–**8**) containing substituted pyridyl–thiazole ligands, [Ru(η^6-*p*-cymene)(L)Cl]Cl (L = N,N-chelating derivatives), have been synthesized and characterized using elemental analysis, infrared, ^{1}H NMR and ^{13}C NMR spectroscopies and mass spectrometry. All these complexes not only display marked cytotoxicity *in vitro* against three different human cancer cell lines (HeLa, A549 and MDA-MB-231), but also exhibit promising anti-metastatic activity at sub-cytotoxic concentrations. Cell cycle analysis shows that the ruthenium(II) complex-induced growth inhibition was mainly caused by S-phase cell cycle arrest. Further protein level analysis suggests that compound **5** may exert antitumor activity via a p53-independent mechanism.

KEYWORDS
anti-metastasis, cytotoxicity, ruthenium(II), synthesis

1 | INTRODUCTION

In the 1960s, the discovery of cisplatin was a great breakthrough for the treatment of cancers with metal-based drugs, and shortly afterwards, a few platinum derivatives (carboplatin and oxaliplatin) were approved for use in the clinical treatment of cancer.[1] Despite the remarkable advances that have been made in the field of chemotherapy, these complexes suffer from severe toxic side effects and acquired drug resistance.[2–5] Therefore, scientists are urgently searching for new bioactive metal complexes, including those of platinum, gold[6] and ruthenium,[7–11] as alternative therapeutics. Obviously, ruthenium-based agents have attracted increasing attention in recent years.[7–11] A large number of anticancer ruthenium complexes have been reported, including arene ruthenium(II) complexes. There are two well-known ruthenium-based anticancer drug leaders, the complexes KP1019 and NAMI-A, which have already entered phase II clinical trials. NAMI-A has shown strong anti-metastasis activity against many mammal tumor cells but almost no cytotoxic effects,[12] while KP1019 is cytotoxic, and has demonstrated its antitumor effects against many human tumor cells by inducing apoptosis.[13]

We are interested in bioactive compounds with dual cytotoxic and anti-metastatic properties, which can effectively enhance anticancer potency by reducing the acquired drug resistance and systematic toxicities generated by using either a cytotoxic or an anti-metastatic agent alone.[14] An anti-metastatic Ru(III) complex with ferrocenylpyridine-NAMI-A has recently been reported to display promising cytotoxic properties, but such ruthenium complexes are sparse in the literature.[15]

Thiazole derivatives are showing promise in a variety of medicinal applications, including those involving their antiproliferative activities.[16–22] Considering properties such as water solubility and coordinate site making for drug development, we introduce a pyridyl moiety to thiazole to form a series of pyridyl–thiazole ligands with different substituent groups, then combine the anti-metastatic property exhibited by the *p*-cymene ruthenium(II) unit with the established antiproliferative

effects of the pyridyl–thiazole ligands. In this paper, we present for the first time the synthesis, characterization, cytotoxicity, anti-metastatic activity and preliminary mechanism of action of a series of novel ruthenium(II) compounds with pyridyl–thiazole ligands.

2 | RESULTS AND DISCUSSION

2.1 | Synthesis and Characterization

The synthesis of arene ruthenium(II) complexes containing pyridyl–thiazole ligands was conducted using the reaction route shown in Scheme 1. Arene–Ru(II) complexes **1–8** were prepared by the reaction of $[Ru(\eta^6\text{-}p\text{-cymene})Cl_2]_2$ with the respective ligands (L^1–L^8) in dried methanol at room temperature for 8 h. All the complexes are red powders, and stable when exposed to moist air. They are freely soluble in dimethylsulfoxide (DMSO), slightly soluble in alcohols and almost insoluble in dichloromethane, chloroform and ethyl acetate.

All complexes were isolated as their chloride salts, and were characterized using elemental analysis, and infrared (IR), ^{1}H NMR and ^{13}C NMR spectroscopies. The elemental analysis data for the complexes are in good agreement with the calculated values. In the IR spectra of the Ru(II)–cymene complexes **1–8**, the bands of stretching vibration of N—H appear in the range 3442–3462 cm^{-1}, and the $\nu_{(Ru—N)}$ bands appear in the range 515–598 cm^{-1}, indicating that the coordination of ligands with $[Ru(\eta^6\text{-}p\text{-cymene})Cl_2]_2$ is derived from two nitrogen atoms in pyridine and thiazole rings, respectively. The $\nu_{(C=N)}$ bands (in the range 1529–1537 cm^{-1}) are shifted to lower wavenumber by about 23 cm^{-1} compared to the free ligands ($\nu_{(C=N)}$ for pyridyl–thiazolo ligands are in the range 1549–1563 cm^{-1}). This similar shifting has also been reported in recent literature.[23] All these phenomena in the IR spectra demonstrate the pyridyl–thiazole ligands are coordinated with ruthenium(II) atoms as an N,N-chelating arrangement.

The ^{1}H NMR spectra of all eight ruthenium(II) complexes show the signals of the η^6-*p*-cymene ring, and the characteristic signals of the thiazole ligands at much higher chemical shifts related to their free form owing to the deshielding effect produced by the arene–ruthenium(II) unit. The signal of pyridine proton

TABLE 1 Cell viability of three human tumor cell lines treated with **1–8** and L^1–L^8 at 30 and 300 μM

	Cell viability (%)					
	HeLa		A549		MDA-MB-231	
Compound	30 μM	300 μM	30 μM	300 μM	30 μM	300 μM
1	7.7	6.8	8.3	9.4	34.3	8.6
2	5.7	6.6	6.7	9.5	16.7	8.1
3	6.6	6.3	6.5	8.3	32.5	6.9
4	4.9	5.6	7.7	7.8	26.1	6.3
5	5.9	7.2	7.3	9.8	9.4	7.9
6	5.9	6.6	7.4	9.0	9.4	5.9
7	7.8	6.3	7.6	10.3	13.3	8.1
8	6.1	6.1	7.4	9.4	13.5	7.0
L^1	57.7	11.4	39.4	32.3	67.6	47.4
L^2	66.1	44.3	42.8	38.1	89.8	65.2
L^3	57.3	39.9	37.5	11.3	64.7	50.3
L^4	61.7	16.5	43.4	14.9	80.4	62.7
L^5	64.2	9.0	46.9	10.3	75.2	51.2
L^6	83.1	5.9	60.7	11.1	87.5	26.1
L^7	59.5	4.2	38.9	40.8	94.1	70.6
L^8	64.3	19.5	49.3	16.4	85.2	54.4
NAMI-A	95.6	86.3	97.4	97.7	100.0	93.5
Cisplatin	52.5	5.0	32.4	14.4	80.8	18.9

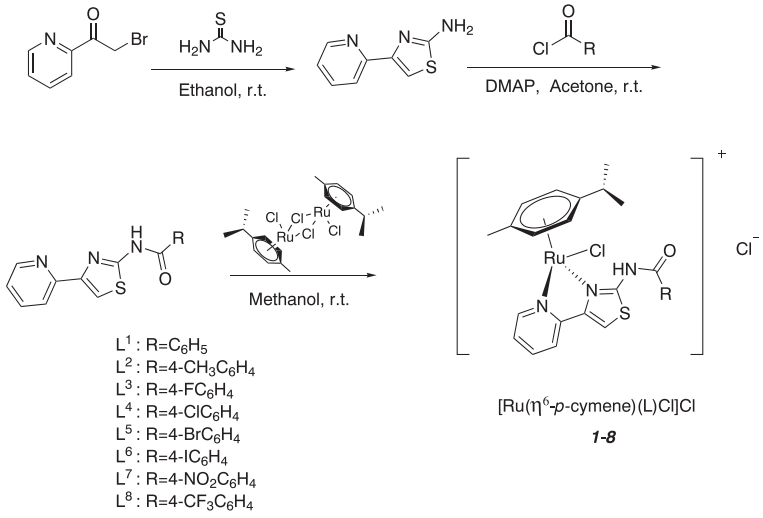

SCHEME 1 Synthetic route to $[Ru(\eta^6\text{-}p\text{-cymene})(L)Cl]Cl$ complexes (**1–8**)

(—CH=N) for free-form ligands is a doublet at around 8.7 ppm, and shifts to around 9.3 ppm after complexation with ruthenium atoms due to the deshielding effect. Similar downfield shifts in ^{1}H NMR spectra have also been reported recently.[11] The ^{13}C NMR spectra of **1**–**8** also show the expected resonance signals.

The mass spectra of all eight ruthenium(II) compounds show the respective molecular fragment ions, $[M - Cl]^{+}$, formed upon loss of chlorine ligands.

2.2 | *In Vitro* Antiproliferative Activity

The antiproliferative properties of the new ruthenium(II) complexes **1**–**8** and of the corresponding ligands L^1–L^8 were screened using MTT assay. Cell viability of all the compounds was determined at doses of 30 and 300 μM against three human cancer cell lines: cervix (HeLa), lung (A549) and triple negative breast (MDA-MB-231). The cell viability data for complexes **1**–**8** and the eight ligands are presented in Table 1 along with the data for NAMI-A and cisplatin for comparison. Figure 1 shows cytotoxicity results for **1**–**8** and L^1–L^8 at doses of 30 and 300 μM against HeLa, A549 and MDA-MB-231 human cancer cell lines for 48 h. The IC_{50} values of some of the complexes against the three cancer lines were obtained, and the data are summarized in Table 2.

On the basis of the data in Table 1 and Figure 1, almost all the complexes show obviously stronger cytotoxicity than the pyridyl–thiazole ligands against the three human cancer cell lines regardless of higher (300 μM) or lower (30 μM) concentrations, confirming that the coordination of the ligands with ruthenium(II) precursor $[Ru(\eta^6\text{-}p\text{-cymene})Cl_2]_2$ can enhance strongly the antiproliferative activity.

Among the eight ruthenium(II)–cymene complexes investigated, five (**2**, **5**, **6**, **7** and **8**) exhibit a stronger antiproliferative activity than their ligands against the three human tumor cells, being even more active than cisplatin,[24,25] which is clinically widely used. Among the five compounds, **5** and **6** exhibit the highest antiproliferative activities against the three tumor cell lines with IC_{50} values of 1.6–3.9 μM. Based on the data analysis, possible structure–activity relationships can be outlined as follows. (i) The type of substituents can have a marked influence on the cytotoxicity; for example, (a) **5**, with the 4-bromophenylpyridyl–thiazole ligand, is among the most active against all the tumor cells and (b) the complexes with withdrawing groups are shown to exhibit marked *in vitro* cytotoxicity towards various human tumor cell lines, which is ligand-dependent – the replacement of one methyl by bromo- or iodo- substituent (**5**, **6**) leads to a high activity enhancement. (ii) However, the

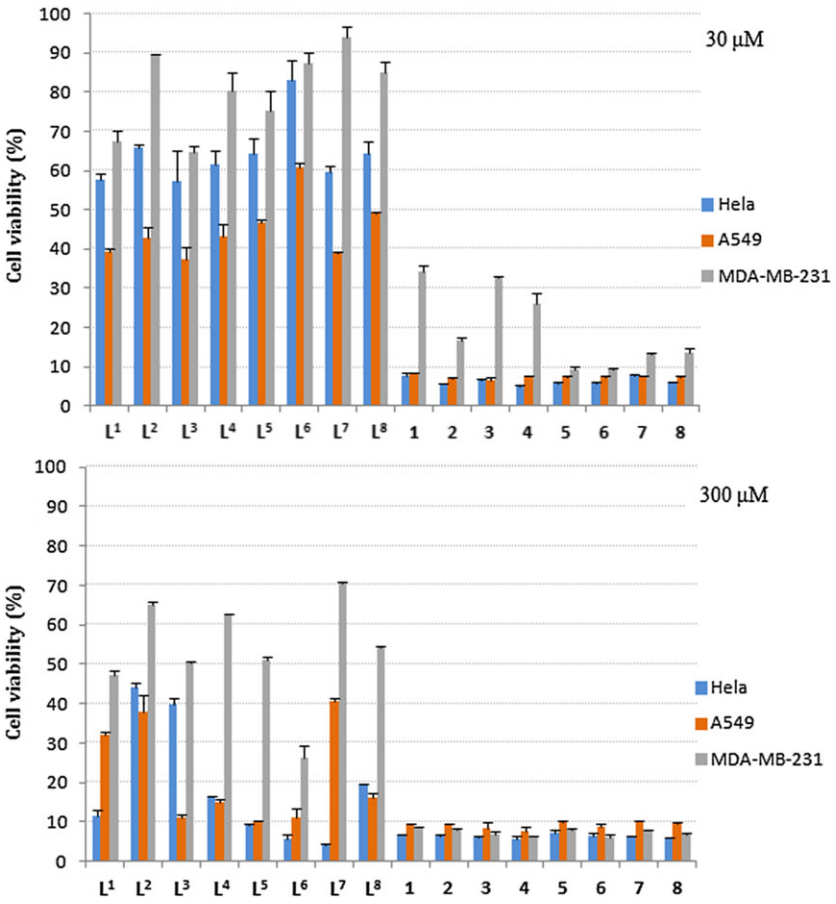

FIGURE 1 Cytotoxicity of **1**–**8** and L^1–L^8 at doses of 30 and 300 μM against three human tumor cell lines (HeLa, A549 and MDA-MB-231) for 48 h

TABLE 2 IC_{50} values of five most potent antiproliferative compounds against three human tumor cell lines

		IC_{50} (μM)		
Compound	**R**	**HeLa**	**A549**	**MDA-MB-231**
2	4-$CH_3C_6H_4$	6.3	5.3	17.5
5	4-BrC_6H_4	3.1	1.6	2.5
6	4-IC_6H_4	2.0	3.9	2.4
7	4-$NO_2C_6H_4$	7.5	4.9	5.3
8	4-$CF_3C_6H_4$	5.1	13.1	4.2
Cisplatin		5.8[1]	17.0[1]	36.1[2]

observations in (i) were not proved; for example, the replacement of bromo- by chloro- or fluoro- substituents usually does not lead to a marked effect on the activity, further studies being required to established clear relationships with the activity. (iii) The highest activity is usually observed for the A549 tumor cells.

2.3 | Scratch Wound Healing Assay

Cells have a natural migration tendency that is a vital process in the growth and safeguarding of tissue functions,[26] which is very essential during embryogenesis, wound healing and development of immune response. Wound healing migration is an established protocol that allows examination of cell migration in response to an artificial wound produced on a cell monolayer.[27] It also takes place in cancer, leading to invasion and metastasis.[28]

In this work, a scratch wound healing assay (48 h) was carried out for determining the anti-migration

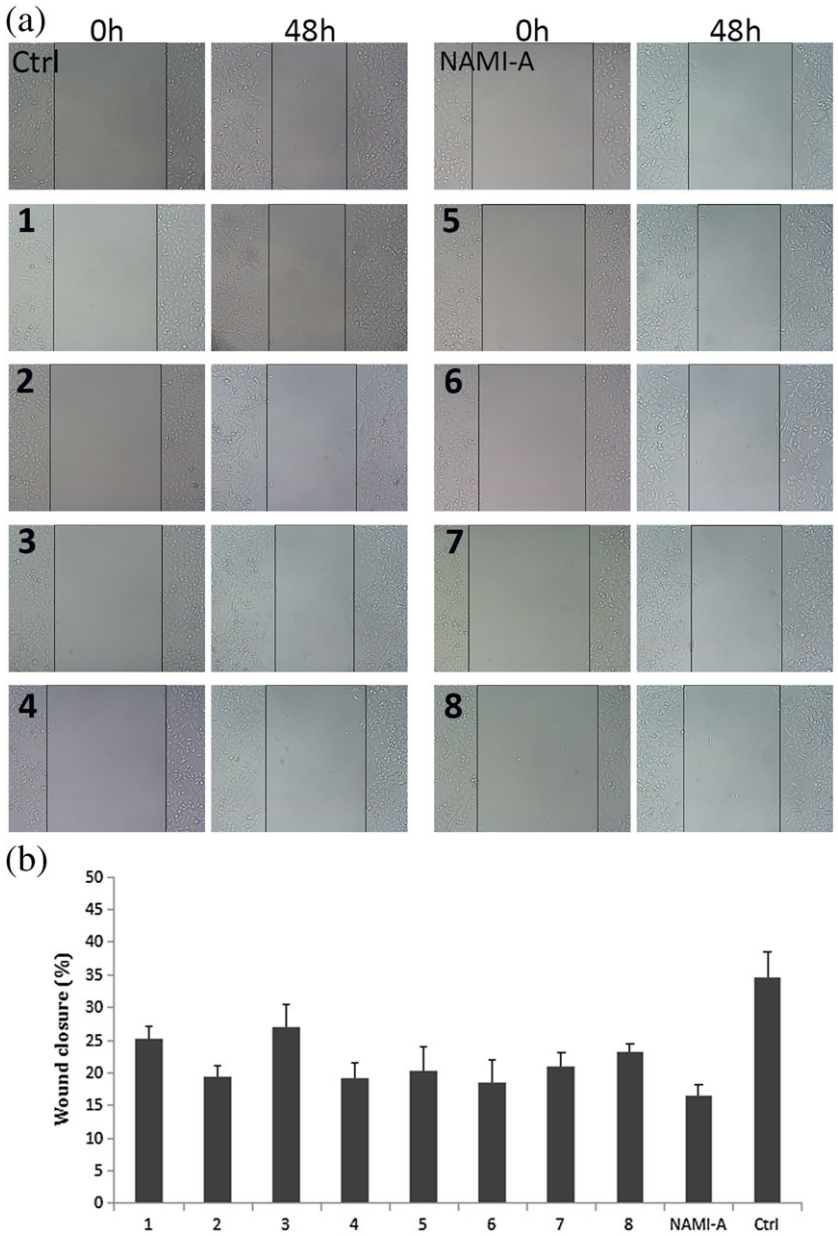

FIGURE 2 (A) Wound healing assay of A549 after treatment with **1**–**8** and NAMI-A at 1.0 μM (culture medium as control). (B) Data analysis of the wound healing rate

activity of **1–8** in highly metastatic A549 lung carcinoma cells. The maximum concentration of **1–8** was restricted to 1.0 μM in order to maintain over 90% viability of the A549 cells after 48 h treatment. NAMI-A has been selected as a positive control because of its well-known significant anti-metastasis activity on human tumor cells.[29]

As depicted in Figure 2, for the A549 cells treated without drugs (control), a distinct cell migration in the wound area was found in 48 h after wounding, with almost 35% wound closure rate. But for complexes **1–8**, a notable inhibition of wound closure was observed, and the wound healing rates decreased to 18–27%, being slower than control. Among the eight complexes, four

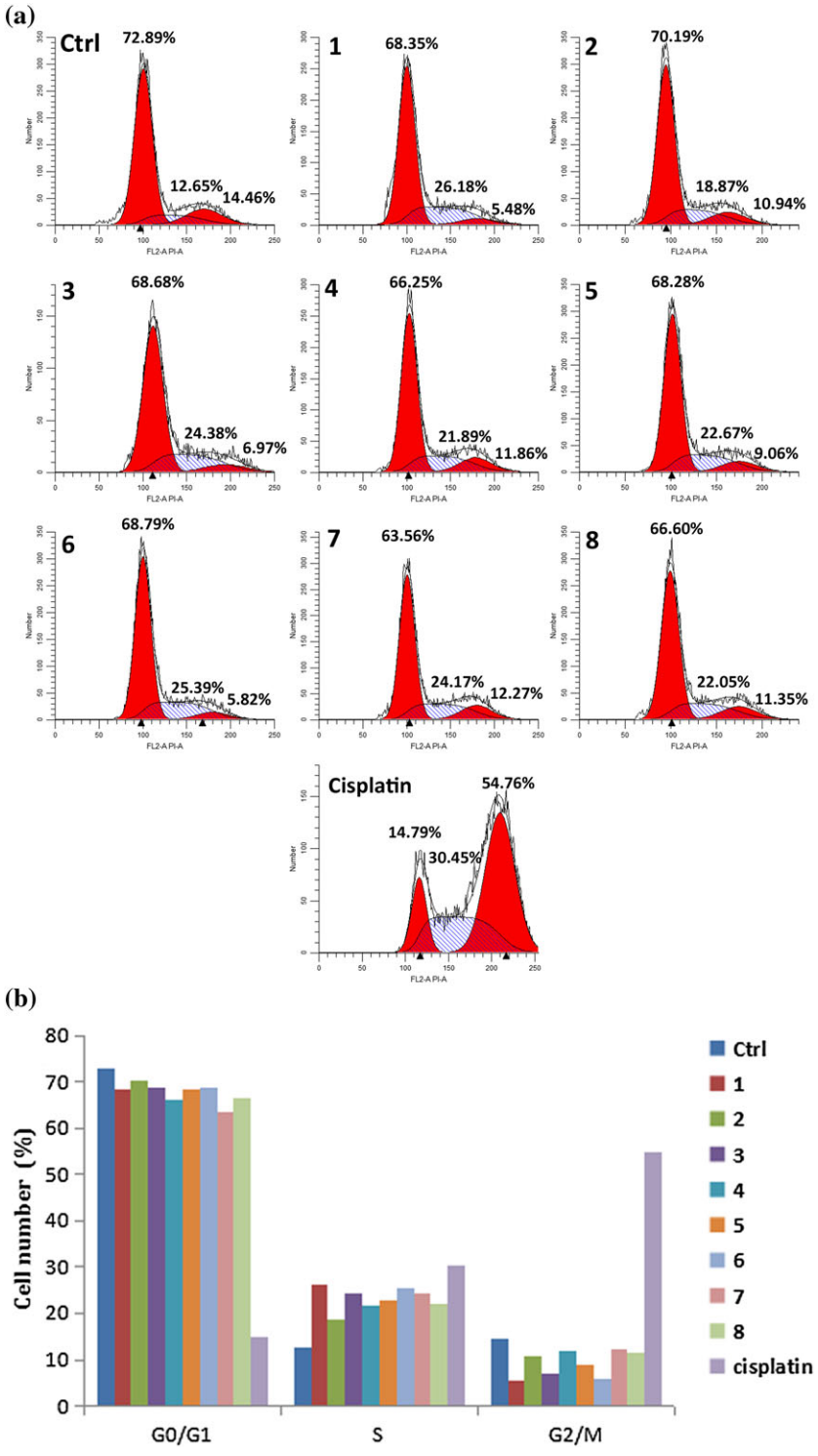

FIGURE 3 (A) Cell cycle distribution of A549 cells after treatment with compounds **1–8** at 5.0 μM. (B) Data analysis of cell cycle arrest

(**2**, **4**, **5** and **6**) exhibit better anti-metastasis activity against A549 cells. Notably, the inhibition rate of wound closure for **6** at 1.0 μM was 18%, being even closer to NAMI-A (wound healing rate of around 17%).

2.4 | Cell Cycle Analysis by Flow Cytometry

The cell cycle is a series of events leading to replication and cell division.[30] Growth inhibition in cancer cells by anticancer drugs could be the result of induction of cell cycle arrest.[31] Therefore, the ability of **1**–**8** to cause cell cycle arrest was investigated to gain more insight into the antiproliferative activity. A549 cells were treated with complexes **1**–**8** for 48 h at 5 μM. Cisplatin was used as a positive control at the same concentration. The cell cycle profiles of treated cells stained with propidium iodide were obtained by flow cytometry analysis and compared with that of an untreated control.

As shown in Figure 3, the cell proportion for all complexes except **2** is beyond 20% at S phase, which is much higher than that of control (12.65%). Almost all the new ruthenium complexes can trigger certain increase of cell proportion at S-phase, accompanied by decrease in the percentage of cells at G0/G1 and G2/M phases, suggesting that the complexes could be cell cycle phase-specific agents. In contrast, cells incubated with cisplatin were arrested at both S-phase and G2/M phase, and cell proportion at G2/M phase was even increased to 54.76%, and this result is in accordance with previous reports that cisplatin is a representative cell cycle phase nonspecific chemotherapeutic drug.[29] The different effect of these two kinds of metal-based complexes on A549 cell cycle may suggest that the series of ruthenium(II) complexes showed a much stronger antitumor effect and led to higher cells arrest at S phase, and the ruthenium(II) complexes may have a mechanism of action different from that of cisplatin or NAMI-A or other typical ruthenium complexes that lack *in vitro* cytotoxicity but possess marked anti-metastasis activity.[29,32,33]

2.5 | Mechanistic Considerations (Western Blot for p53)

TP53 tumor suppressor gene is involved in the mediation of cellular DNA repair, apoptosis induction and cell cycle arrest.[34] TP53 has been found altered in more than approximately 50% of human malignancies, and the mutation of p53 genes or over-expression of p53 negative regulators often make many cancer patients resistant to drugs that act via p53-dependent pathways.[35] And the chemo-resistance of some cancer cell lines has been shown to be due to mutated TP53-encoding genes or deficient p53 protein levels, which are less effective in inducing apoptosis even when significant DNA damage has occurred.[36,37] Therefore, p53 is a highly attractive and promising therapeutic target for cancer treatment. Traditional platinum compounds such as cisplatin and oxaliplatin exert their antiproliferative activity by increasing the expression of p53 protein.[38,39] Those anticancer agents via a p53-independent mechanism could be promising drug candidates against drug-resistant cancers. In light of this, it is necessary to investigate whether the cytotoxicity of the newly synthesized ruthenium compounds is p53-dependent or p53-independent.

To determine whether the cytotoxicity of the compounds is dependent on or independent of p53, we chose complex **5** with good cytotoxicity to analyze the levels of p53 protein in A549 cells for 48 h, with cisplatin as a positive control. GAPDH (glyceraldehyde-3-phosphate dehydrogenase) levels were determined in the same membranes as a total protein loading control. In addition, we measured the p53 expression in A549 cells after different exposure concentrations (2.0 and 5.0 μM) to **5** and cisplatin.

As shown in Figure 4, p53 can remain stable after treatment with **5** at 2.0 μM, but with an increase of the concentration of **5**, we observed a slight down-regulation in p53 levels at 5.0 μM, probably due to cell death and protein loss. For cisplatin, p53 expression in A549 cells

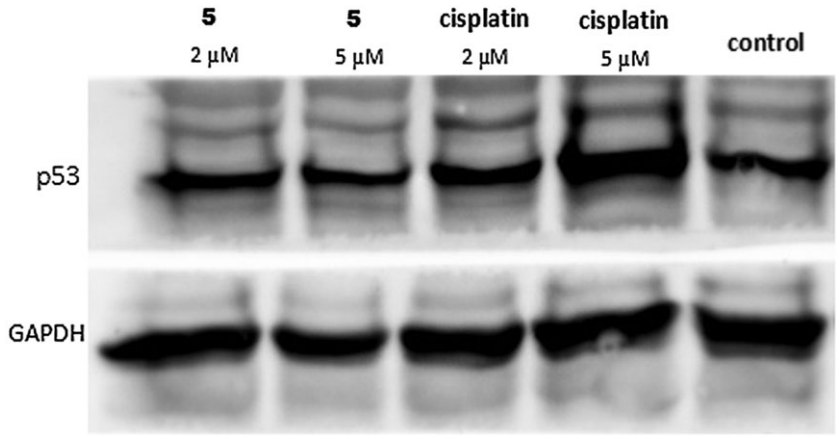

FIGURE 4 p53 protein levels after short-term incubation of A549 cells with compound **5** and cisplatin at 2.0 and 5.0 μM. GAPDH levels were determined in the same membranes as a total protein loading control

remained at basal level at 2.0 μM, but showed an obvious increase at higher concentration (5.0 μM), indicating a concentration-dependent up-regulation of p53 mechanism as expected.[38,39] This suggests that the new ruthenium(II) complex **5** exerts anticancer activity through a p53-independent mechanism,[37,40] unlike RAPTA-C,[41] RM175[42] or cisplatin via a p53-dependent mechanism. The results hold promise for treatment of cancers that are drug-resistant due to their dysfunctional p53 status.

3 | CONCLUSIONS

In this work we have reported the synthesis of a series of new ruthenium(II)–cymene complexes coordinated by pyridyl–thiazole derivatives. All compounds were characterized using elemental analysis, and IR, ^{1}H NMR and ^{13}C NMR spectroscopies.

The *in vitro* cytotoxic activity was evaluated by MTT assay against three human cancer cell lines (HeLa, A549 and MDA-MB-231). Ruthenium(II) complexes **2**, **5**, **6**, **7** and **8** display strong cytotoxicity against the three cell lines with cell viability below 16.7%. Complexes **1**, **3** and **4** show weaker antiproliferative activity against MDA-MB-231 cells at a dose of 30 μM.

Cell cycle arrest was also investigated by flow cytometry for the antiproliferative mechanism. All the new ruthenium complexes triggered certain increase of A549 cell proportion at S phase, accompanied by a decrease in the percentage of cells at G2/M phase, indicating that **1**–**8** may be cell cycle S-phase-specific agents.

Scratch wound healing assay was used to investigate the migration of A549 human cancer cells for anti-metastasis effect. The results indicate that compounds **2**, **4**, **5** and **6** exhibit better anti-metastasis activity in A549 cells. Especially, **6** possesses the best anti-metastatic potential.

According to the data of antiproliferative and anti-metastasis activity, the ruthenium(II)–cymene complexes containing pyridyl–thiazole ligands **2**, **5** and **6** exhibit promising dual anti-metastatic and cytotoxic properties.

Furthermore, protein level research for p53 was carried out by western blot analysis, suggesting that the new ruthenium complex **5** exerts its antiproliferation activity via a p53-independent mechanism, unlike cisplatin or some other traditional ruthenium complexes. These results hold promise for treatment of cancers that are drug resistant due to their mutated p53 or p53-null status. The studies also pave the way for the development of arene–ruthenium(II) complexes as the next generation of metal-based anticancer drugs.

4 | EXPERIMENTAL

4.1 | Materials and Physical Measurements

$RuCl_3 \cdot 3H_2O$, 2-(bromoacetyl)pyridine hydrobromide and 4-dimethylaminopyridine were purchased from Meryer (Shanghai) Chemical Technology Co. Ltd. [Ru(η^6-*p*-cymene)Cl_2]$_2$ and the ligands (L^1–L^8) were synthesized using literature methods.[43,44] NAMI-A was prepared according to a patented procedure.[45] The acyl chloride, thiourea and all other chemical reagents were obtained from Sinopharm Chemical Reagent Co. Ltd, China, and were used as received. All biological materials were purchased from Gibco. Elemental analyses were performed with a PerkinElmer 2400 analyzer, series II. IR spectra were recorded from 4000 to 400 cm^{-1} with a Bruker Vertex 70 FT-IR spectrophotometer using KBr pellets; only significant bands are cited in the text. NMR spectra were recorded with a Bruker AM-400 spectrometer. ^{1}H and ^{13}C chemical shifts are reported relative to tetramethylsilane. Electrospray ionization (ESI) mass spectra were recorded in positive mode (+) with a Bruker SolariX 7.0 T Fourier transform mass spectrometer.

4.2 | Synthesis of [Ru(η6-p-cymene)(L)Cl]Cl Complexes

4.2.1 | Synthesis of [Ru(η^6-*p*-cymene)(L^1)Cl]Cl (1)

An amount of 180 mg (0.3 mmol) of [Ru(η^6-*p*-cymene)Cl_2]$_2$ was added to a dried methanol (12 ml) solution of 141 mg (0.5 mmol) of L^1, and the mixture was stirred at room temperature for 8 h. Then the mixture was filtered to remove the insoluble material. Ethyl acetate (500 ml) was added to the mixture. Two days later, red powders were obtained. The resulting solid was then washed several times with a mixed solvent of dichloromethane and ethyl acetate (10:1). The final product was then dried *in vacuo* at 60 °C for 6 h to remove residual solvents, and the red powders were obtained. Yield: 28.8%. IR (KBr, ν, cm^{-1}): 3443 (N—H), 1677 (C=O), 1609, 1533 (C=N), 598, 521 (Ru—N). Anal. Calcd for $C_{25}H_{25}Cl_2N_3ORuS$ (%): C 51.11, H 4.29, N 7.15, S 5.46. Found (%): C 51.36, H 4.26, N 6.98, S 5.52. ^{1}H NMR (400 MHz, DMSO-d_6, δ, ppm): 9.31 (d, J = 5.1 Hz, 1H, Ar–*H*), 8.14 (m, 5H, Ar–*H*), 7.59 (m, 4H, Ar–*H*), 6.68 (d, J = 5.2 Hz 1H, —C_6H_4—), 6.13 (d, J = 5.2 Hz, 1H,—C_6H_4—), 5.99 (d, J = 5.2 Hz, 2H, —C_6H_4—), 2.47 (m, 1H, $CH_3C_6H_4CH(CH_3)_2$), 2.25 (s, 3H, $CH_3C_6H_4CH(CH_3)_2$), 0.91 (d, J = 6.8 Hz, 3H, $CH_3C_6H_4CH(CH_3)_2$), 0.87 (d, J = 6.8 Hz, 3H, $CH_3C_6H_4CH(CH_3)_2$). ^{13}C NMR (150 MHz,

DMSO-d_6, δ, ppm): 169.31, 156.95, 151.50, 140.89, 133.09, 131.74, 129.28(3C), 127.02, 135.01, 123.86, 123.01, 122.22, 117.64, 101.83, 100.60, 87.20, 86.26, 81.71, 80.27, 30.93, 22.65, 22.35, 19.7. ESI-MS (+ mode, in MeOH): m/z 552 $[M - Cl]^+$.

4.2.2 | Synthesis of [Ru(η^6-*p*-cymene)(L^2)Cl]Cl (2)

Compound **2** was prepared analogously by following the method and conditions described for **1**. Red powders were obtained. Yield: 23.1%. IR (KBr, ν, cm^{-1}): 3451 (N—H), 1678 (C=O), 1604, 1536 (C=N), 598, 522 (Ru—N) cm^{-1}. Anal. Calcd for $C_{26}H_{27}Cl_2N_3ORuS$ (%): C 51.91, H 4.52, N 6.99, S 5.33. Found (%): C 51.74, H 4.47, N 7.14, S 5.42. ^{1}H NMR (400 MHz, DMSO-d_6, δ, ppm): 9.35 (d, J = 5.1 Hz, 1H, Ar—*H*), 8.27–8.17 (m, 3H, Ar—*H*), 8.01(d, J = 8.1 Hz, 2H, Ar—*H*), 7.61 (m, 1H, Ar—*H*), 7.41(d, J = 8.1 Hz, 2H, Ar—*H*), 6.65 (d, J = 5.2 Hz, 1H, —C_6H_4—), 6.18 (d, J = 5.2 Hz, 1H, —C_6H_4—), 6.02 (d, J = 5.2 Hz, 2H, —C_6H_4—), 2.47 (m, 1H, $CH_3C_6H_4CH(CH_3)_2$), 2.44(s, 3H, Ar—CH_3), 2.27(s, 3H, $CH_3C_6H_4CH(CH_3)_2$), 0.92 (d, J = 6.8 Hz, 3H, $CH_3C_6H_4CH(CH_3)_2$), 0.87 (d, J = 6.8 Hz, 3H, $CH_3C_6H_4CH(CH_3)_2$). ^{13}C NMR (150 MHz, DMSO-d_6, δ, ppm): 165.91, 156.99, 151.45, 143.67, 142.31, 140.98, 129.93(2C), 129.30(2C), 127.10, 124.40, 123.29, 122.15, 101.95, 100.56, 87.22, 86.26, 81.74, 80.23, 30.91, 22.67, 22.35, 21.98, 19.78. ESI-MS (+ mode, in MeOH): m/z 566 $[M - Cl]^+$.

4.2.3 | Synthesis of [Ru(η^6-*p*-cymene)(L^3)Cl]Cl (3)

Compound **3** was prepared analogously by following the method and conditions described for **1**. Red powders were obtained. Yield: 18.9%. IR (KBr, ν, cm^{-1}): 3451 (N—H), 1681 (C=O), 1609, 1533 (C=N), 584, 517 (Ru—N). Anal. Calcd for $C_{25}H_{24}Cl_2FN_3ORuS$ (%): C 49.59, H 4.00, N 6.94, S 5.29. Found (%): C 49.42, H 4.19, N 6.74, S 5.15. ^{1}H NMR (400 MHz, DMSO-d_6, δ, ppm): 9.32 (d, J = 5.6 Hz, 1H, Ar—*H*), 8.22–8.18 (m, 4H, Ar—*H*), 8.11 (d, J = 7.7 Hz, 1H,Ar—*H*), 7.56 (t, J = 5.6 Hz, 1H, Ar—*H*), 7.40 (t, J = 8.7 Hz, 2H, Ar—*H*), 6.68 (d, J = 5.8 Hz, 1H, —C_6H_4—), 6.13 (d, J = 5.8 Hz, 1H, —C_6H_4—), 5.98 (d, J = 6.1 Hz, 2H, —C_6H_4—), 2.47 (m, 1H, $CH_3C_6H_4CH(CH_3)_2$), 2.26 (s, 3H, $CH_3C_6H_4CH(CH_3)_2$), 0.92 (d, J = 6.9 Hz, 3H, $CH_3C_6H_4CH(CH_3)_2$), 0.87 (d, J = 6.9 Hz, 3H, $CH_3C_6H_4CH(CH_3)_2$). ^{13}C NMR (150 MHz, DMSO-d_6, δ, ppm): 165.76, 164.13, 162.13, 156.84, 151.59, 146.59, 140.70, 132.26, 127.00, 124.87, 122.80, 116.15, 114.29, 111.19, 106.77, 101.50, 100.59, 87.17, 86.23, 81.61, 80.14, 30.99, 22.63, 22.34, 19.76. ESI-MS (+ mode, in MeOH): m/z 570 $[M - Cl]^+$.

4.2.4 | Synthesis of [Ru(η^6-*p*-cymene)(L^4)Cl]Cl (4)

Compound **4** was prepared analogously by following the method and conditions described for **1**. Red powders were obtained. Yield: 29.3%. IR (KBr, ν, cm^{-1}): 3446 (N—H), 1680 (C=O), 1608, 1533 (C=N), 586, 519 (Ru—N). Anal. Calcd for $C_{25}H_{24}Cl_3N_3ORuS$ (%): C 48.28, H 3.89, N 6.76, S 5.16. Found (%): C 47.93, H 3.74, N 6.61, S 5.13. ^{1}H NMR (400 MHz, DMSO-d_6, δ, ppm): 9.31 (d, J = 3.8 Hz, 1H, Ar—*H*), 8.28–8.05 (m, 5H, Ar—*H*), 7.64 (d, J = 8.3 Hz, 2H, Ar—*H*), 7.55 (t, J = 5.6 Hz, 1H, Ar—*H*), 6.65 (d, J = 5.5 Hz, 1H, —C_6H_4—), 6.11 (d, J = 5.5 Hz, 1H, —C_6H_4—), 5.97 (d, J = 5.5 Hz, 2H, —C_6H_4—), 2.46 (m, 1H, $CH_3C_6H_4CH(CH_3)_2$), 2.25 (s, 3H, $CH_3C_6H_4CH(CH_3)_2$), 0.91 (d, J = 6.6 Hz, 3H, $CH_3C_6H_4CH(CH_3)_2$), 0.86 (d, J = 6.6 Hz, 3H, $CH_3C_6H_4CH(CH_3)_2$). ^{13}C NMR (150 MHz, DMSO-d_6, δ, ppm): 170.67, 155.76, 152.07, 147.46, 146.16, 140.08, 136.78, 130.96(2C), 129.02(2C), 125.87, 124.06, 123.84, 121.86, 101.37, 100.57, 86.99, 86.29, 81.32, 79.93, 30.92, 22.39, 22.30, 19.54. ESI-MS (+ mode, in MeOH): m/z 586 $[M - Cl]^+$.

4.2.5 | Synthesis of [Ru(η^6-*p*-cymene)(L^5)Cl]Cl (5)

Compound **5** was prepared analogously by following the method and conditions described for **1**. Red powders were obtained. Yield: 31.2%. IR (KBr, ν, cm^{-1}): 3462 (N—H), 1686 (C=O), 1610, 1537 (C=N), 593, 516 (Ru—N). Anal. Calcd for $C_{25}H_{24}Cl_2BrN_3ORuS$ (%): C 45.06, H 3.63, N 6.31, S 4.81. Found (%): C 44.86, H 3.39, N 6.34, S 4.62. ^{1}H NMR (400 MHz, DMSO-d_6, δ, ppm): 9.31 (d, J = 5.4 Hz, 1H, Ar—*H*), 8.30–8.02 (m, 3H, Ar—*H*), 7.97–7.91 (m, 4H, Ar—*H*), 7.54 (t, J = 5.6 Hz, 1H, Ar—*H*), 6.64 (d, J = 5.2 Hz, 1H, —C_6H_4—), 6.11 (d, J = 5.2 Hz, 1H, —C_6H_4—), 5.96 (d, J = 5.2 Hz, 2H, —C_6H_4—), 2.46 (m, 1H, $CH_3C_6H_4CH(CH_3)_2$), 2.25 (s, 3H, $CH_3C_6H_4CH(CH_3)_2$), 0.92 (d, J = 6.8 Hz, 3H, $CH_3C_6H_4CH(CH_3)_2$), 0.88 (d, J = 6.8 Hz, 3H, $CH_3C_6H_4CH(CH_3)_2$). ^{13}C NMR (150 MHz, DMSO-d_6, δ, ppm): 169.38, 156.64, 151.81, 146.38, 140.66, 138.52, 132.16(2C), 131.26(2C), 127.02, 126.62, 126.01, 123.94, 122.79, 101.61, 101.24, 89.22, 86.24, 81.63, 80.15, 30.94, 22.57, 22.40, 19.78. ESI-MS (+ mode, in MeOH): m/z 629 $[M - Cl]^+$.

4.2.6 | Synthesis of [Ru(η^6-*p*-cymene)(L^6)Cl]Cl (6)

Compound **6** was prepared analogously by following the method and conditions described for **1**. Red powders were obtained. Yield: 34.6%. IR (KBr, ν, cm^{-1}): 3442 (N—H), 1676 (C=O), 1609, 1529 (C=N), 588, 519 (Ru—N). Anal.

Calcd for $C_{25}H_{24}Cl_2IN_3ORuS$ (%): C 42.09, H 3.39, N 5.89, S 4.49. Found (%): C 41.76, H 3.28, N 5.56, S 4.30. ^{1}H NMR (400 MHz, DMSO-d_6, δ, ppm): 9.31 (d, J = 5.2 Hz, 1H, Ar—*H*), 8.19–8.08 (m, 5H, Ar—*H*), 7.77 (d, J = 8.3 Hz, 2H, Ar—*H*), 7.54 (t, J = 5.6 Hz, 1H, Ar—*H*), 6.66 (d, J = 5.2 Hz, 1H, —C_6H_4—), 6.11 (d, J = 5.2 Hz, 1H, —C_6H_4—), 5.96 (d, J = 5.2 Hz, 2H, —C_6H_4—), 2.47 (m, 1H, $CH_3C_6H_4CH(CH_3)_2$), 2.25 (s, 3H, $CH_3C_6H_4CH(CH_3)_2$), 0.92 (d, J = 6.7 Hz, 2H, $CH_3C_6H_4CH(CH_3)_2$), 0.88 (d, J = 6.8 Hz, 3H, $CH_3C_6H_4CH(CH_3)_2$). ^{13}C NMR (150 MHz, DMSO, δ, ppm): 169.40, 156.81, 151.76, 146.55, 140.75, 138.02(2C), 134.96, 132.73, 131.10(2C), 126.79, 123.54, 122.88, 106.79, 101.54, 100.44, 87.19, 86.25, 81.73, 80.14, 30.92, 22.59, 22.37, 19.76. ESI-MS (+ mode, in MeOH): m/z 677 $[M - Cl]^+$.

4.2.7 | Synthesis of [Ru(η^6-*p*-cymene)(L^7)Cl]Cl (7)

Compound **7** was prepared analogously by following the method and conditions described for **1**. Red powders were obtained. Yield: 20.7%. IR (KBr, ν, cm^{-1}): 3462 (N—H), 1679 (C=O), 1608, 1535 (C=N), 584, 515 (Ru—N). Anal. Calcd for $C_{25}H_{24}Cl_2N_4O_3RuS$ (%): C 47.47, H 3.82, N 8.86, S 5.07. Found (%): C 47.37, H 3.36, N 8.79, S 4.91. ^{1}H NMR (400 MHz, DMSO-d_6, δ, ppm): 9.32 (d, J = 5.3 Hz, 1H, Ar—*H*), 8.41 (m, 4H, Ar—*H*), 8.17 (d, J = 7.7 Hz, 1H, Ar—*H*), 8.13–8.03 (m, 2H, Ar—*H*), 7.53 (t, J = 5.6 Hz, 1H, Ar—*H*), 6.65 (d, J = 5.6 Hz, 1H, —C_6H_4—), 6.11 (d, J = 5.6 Hz, 1H, —C_6H_4—), 5.97 (d, J = 5.7 Hz, 2H, —C_6H_4—), 2.47 (m, 1H, $CH_3C_6H_4CH(CH_3)_2$), 2.24 (s, 3H, $CH_3C_6H_4CH(CH_3)_2$), 0.92 (d, J = 6.8 Hz, 3H, $CH_3C_6H_4CH(CH_3)_2$), 0.88 (d, J = 6.8 Hz, 3H, $CH_3C_6H_4CH(CH_3)_2$). ^{13}C NMR (151 MHz, DMSO-d_6, δ, ppm): 169.58, 156.21, 152.25, 149.27, 148.01, 146.24, 140.29, 130.31(2C), 126.18, 124.18(2C), 123.51, 122.21, 118.97, 100.6, 100.0, 86.51, 86.22, 81.76, 80.05, 31.00, 22.43(2C), 19.70. ESI-MS (+ mode, in MeOH): m/z 597 $[M - Cl]^+$.

4.2.8 | Synthesis of [Ru(η^6-*p*-cymene)(L^8)Cl]Cl (8)

Compound **8** was prepared analogously by following the method and conditions described for **1**. Red powders were obtained. Yield: 23.8%. IR (KBr, ν, cm^{-1}): 3462 (N—H), 1683 (C=O), 1607, 1530 (C=N), 574, 524 (Ru—N). Anal. Calcd for $C_{26}H_{24}Cl_2F_3N_3ORuS$ (%): C 47.64, H 3.69, N 6.41, S 4.89. Found (%): C 47.38, H 3.49, N 6.29, S 4.53. ^{1}H NMR (400 MHz, DMSO-d_6, δ, ppm): 9.32 (d, J = 5.0 Hz, 1H, Ar—*H*), 8.35 (d, J = 8.0 Hz, 2H, Ar—*H*), 8.24–8.03 (m, 3H, Ar—*H*), 7.93 (d, J = 8.1 Hz, 2H, Ar—*H*), 7.53 (t, J = 5.6 Hz, 1H, Ar—*H*), 6.67 (d, J = 5.2 Hz, 1H, —C_6H_4—), 6.11 (d, J = 5.2 Hz, 1H, —C_6H_4—), 5.97 (d, J = 5.2 Hz, 2H, —C_6H_4—), 2.24 (s, 3H, $CH_3C_6H_4CH(CH_3)_2$), 2.47 (m, 1H, $CH_3C_6H_4CH(CH_3)_2$), 0.92 (d, J = 6.7 Hz, 3H, $CH_3C_6H_4CH(CH_3)_2$), 0.88 (d, J = 6.7 Hz, 3H, $CH_3C_6H_4CH(CH_3)_2$). ^{13}C NMR (150 MHz, DMSO-d_6, δ, ppm): 169.62, 156.89, 152.03, 146.34, 140.85, 131.45, 129.98(2C), 127.27, 126.76, 126.05(2C), 125.46, 123.66, 122.93, 120.92, 101.94, 101.54, 89.32, 86.67, 82.01, 80.42, 31.00, 22.59, 22.47, 19.86. ESI-MS (+ mode, in MeOH): m/z 620 $[M - Cl]^+$.

4.3 | *In Vitro* Antiproliferative Activity

The following three human cancer cell lines were used for biological assays: cervical carcinoma (HeLa), lung carcinoma (A549) and triple negative breast carcinoma (MDA-MB-231). All cell lines were maintained in either F12 K medium (A549) or Dulbecco's modified Eagle medium (HeLa and MDA-MB-231) supplemented with fetal bovine serum (10%), penicillin (100 U ml^{-1}) and streptomycin (50 U ml^{-1}) at 37 °C in a CO_2 incubator (95% relative humidity, 5% CO_2). All biological materials were purchased from Gibco.

The complexes were dissolved in DMSO at a concentration of 20 mM as stock solution, and diluted in culture medium at various concentrations (0.036–20 μM) as working solutions. To avoid DMSO toxicity, the concentration of DMSO was less than 0.1% (v/v) in all experiments.[46]

The cancer cells in exponential phase were digested with trypsin, and seeded into a 96-well plate. Twelve hours later, cancer cells were exposed to drugs at various concentrations in medium for 48 h. Upon completion of incubation for 48 h, MTT dye solution (10 μl, 5 mg ml^{-1}) was added to each well. After 4 h incubation, all the solution inside each well was sucked out carefully and then DMSO (120 μl) was added to solubilize the MTT formazan. The absorbance of each well was measured using a microplate spectrophotometer at a wavelength of 570 nm. Cell viability and the dose causing 50% inhibition of cell growth (IC_{50}) were determined from the curve of inhibiting percentage versus dose.

4.4 | Scratch Wound Healing Assay

A vertical line with a marker pen was first drawn on the back of a 24-well plate for retention. Lung carcinoma cells (A549) in exponential phase were digested with trypsin, and then seeded into a 24-well plate (5×10^5 cells per well), and grown in 5% CO_2 at 37 °C for 12 h. Cell monolayers were wounded with a sterile 100 μl pipette tip and washed with growth medium to remove detached cells from the plates and immediately photographed under a

microscope. Cells were exposed to compound-containing medium (not containing fetal bovine serum) at a concentration of 1.0 μM and incubated at 37 °C in a saturated humidity, 5% CO_2 incubator, and the cells were photographed at 6 and 48 h using an Olympus IX51 microscope (Tokyo, Japan) and a digital camera.

4.5 | Cell Cycle Analysis

Lung carcinoma cells (A549) were digested in exponential phase with trypsin, then seeded into a 6-well plate at density of 3×10^6, and grown in an atmosphere of 5% CO_2 at 37 °C. Twelve hours later, cells were exposed to compound-containing medium at a concentration of 5.0 μM and incubated at 37 °C in a saturated humidity, 5% CO_2 incubator. After 48 h of incubation, the culture medium was discarded, and cells were collected by centrifugation. The cells was washed twice with phosphaye-buffered saline (PBS), and centrifuged. The PBS was discarded, and 300 μl of DNA staining solution and 10 μl of permeabilization solution were added it, then the cell suspension was vortexed and incubated for 30 min at 37 °C, then detected by flow cytometry.

4.6 | Protein Extraction and Western Blot for p53

Lung carcinoma cells (A549) were grown on 6-well plates and treated with 5 and cisplatin at concentrations of 2.0 and 5.0 μM and incubated at 37 °C, 5% CO_2 for 24 h. The A549 cells were lysed with lysis buffer. The cell lysate were then transferred to separate 2 ml tubes and sonicated for 10 s. The samples were then centrifuged at 13000 rpm, 4 °C for 5 min. The supernatant liquid containing the proteins was collected and the total protein content of each sample was then quantified via Bradford's assay. Thirty micrograms of protein from each sample was reconstituted in loading buffer (5% DDT, 1× protein loading dye) and heated at 95 °C for 5 min. The protein mixtures were resolved on a 10% SDS–PAGE gel by electrophoresis and transferred to a nitrocellulose membrane. Equal loading of protein was confirmed by comparison with GAPDH. Immunoblotting for p53 was done using anti-human p53 antibodies. The protein bands were visualized via enhanced chemiluminescence imaging (PXi, Syngene).

ACKNOWLEDGMENTS

This work was supported by the National Natural Science Foundation of China (no. 81102311), the Natural Science Foundation of Hubei Province of China (no. 2016CFB433) and the Fundamental Research Funds for the Central Universities of China (no. 2015TS131).

ORCID

Xianmei Shang http://orcid.org/0000-0002-8616-2419

REFERENCES

[1] L. Kelland, *Nat. Rev. Cancer* **2007**, *7*, 573.

[2] S. Dasari, P. B. Tchounwou, *Eur. J. Pharmacol.* **2014**, *740*, 364.

[3] L. Amable, *Pharm. Res.* **2016**, *106*, 27.

[4] S. van Zutphen, J. Reedijk, *Coord. Chem. Rev.* **2005**, *249*, 2845.

[5] P. C. A. Bruijnincx, P. J. Sadler, *Curr. Opin. Chem. Biol.* **2008**, *12*, 197.

[6] R. W. Y. Sun, C. M. Che, *Coord. Chem. Rev.* **2009**, *253*, 1682.

[7] M. J. Clarke, F. Zhu, D. R. Frasca, *Chem. Rev.* **1999**, *99*, 2511.

[8] Y. He, H. Xue, W. Zhang, L. Wang, G. Xiang, X. Shang, *J. Organometal. Chem.* **2017**, *842*, 82.

[9] D. Chen, V. Milacic, M. Frezza, Q. P. Dou, *Curr. Pharm. Des.* **2009**, *15*, 777.

[10] G. Sava, A. Bergamo, P. J. Dyson, *Dalton Trans.* **2011**, *40*, 9069.

[11] A. Grozav, O. Balacescu, L. Balacescu, T. Cheminel, N. L. Berindan, B. Therrien, *J. Med. Chem.* **2015**, *58*, 8475.

[12] E. S. Antonarakis, A. Emadi, *Cancer Chemother. Pharmacol.* **2010**, *66*, 1.

[13] C. G. Hartinger, M. A. Jakupec, S. Zorbas-Seifried, M. Groessl, A. Egger, W. Berger, H. Zorbas, P. J. Dyson, B. K. Keppler, *Chem. Biodiversity* **2008**, *5*, 2140.

[14] G. Gasparini, R. Longo, M. Fanelli, B. A. Teicher, *J. Clin. Oncol.* **2005**, *23*, 1295.

[15] C. Wu, S. W. Chang, K. E. Prosser, A. W. Y. Leung, S. Santacruz, T. Jang, J. R. Thompson, D. T. T. Yapp, J. J. Warren, M. B. Bally, T. V. Beischlag, C. J. Walsby, *Inorg. Chem.* **2016**, *55*, 177.

[16] A. Grozav, L. I. Găină, V. Pileczki, O. Crisan, L. Silaghi-Dumitrescu, B. Therrien, V. Zaharia, I. Berindan-Neagoe, *Int. J. Mol. Sci.* **2014**, *15*, 22059.

[17] M. K. Dahlgren, A. B. Garcia, A. A. Hare, J. Tirado-Rivest, L. Leng, R. Bucala, W. L. Jordensen, *J. Med. Chem.* **2012**, *55*, 10148.

[18] B. E. Sleebs, W. J. A. Kersten, S. Kulasegaram, G. Nikolakopoulos, E. Hatzis, R. M. Moss, J. P. Parisot, P. E. Czabotar, W. D. Fairlie, E. F. Lee, J. M. Adams, L. Chen, M. F. Delft, K. N. Lowes, A. Wei, D. C. S. Huang, P. M. Colman, L. P. Street, J. B. Baell, K. Watson, G. Lessene, *J. Med. Chem.* **2013**, *56*, 5514.

[19] A. Andreani, S. Burnelli, M. Granaiola, A. Leoni, A. Locatelli, R. Morigi, M. Rambaldi, L. Varoli, N. Calonghi, C. Cappadone, G. Farruggia, M. Zini, C. Stefanelli, L. Masotti, L. M. Radin, N. S. Radin, R. H. Shoemaker, *J. Med. Chem.* **2008**, *51*, 809.

[20] C. J. Thomas, M. M. McCormick, C. Vialas, Z. F. Tao, C. J. Leitheiser, M. J. Rishel, X. Wu, S. M. Hecht, *J. Am. Chem. Soc.* **2002**, *124*, 3875.

[21] A. Ignat, T. Lovasz, M. Vasilescu, E. Fischer-Fodor, C. B. Tatomir, C. Cristea, L. Silaghi-Dumitrescu, V. Zaharia, *Archiv. Pharm.* **2012**, *345*, 574.

[22] S. Zheng, Q. Zhong, Y. Xi, M. Mottama, Q. Zhang, R. L. Schroeder, J. Sridhar, L. He, H. McFerrin, G. D. Wang, *J. Med. Chem.* **2014**, *57*, 6653.

[23] M. Frik, A. Martínez, B. T. Elie, O. Gonzalo, D. R. Mingo, M. Sanau, R. S. Delgado, T. Sadhukha, S. Prabha, J. W. Ramos, I. Marzo, M. Contel, *J. Med. Chem.* **2014**, *57*, 9995.

[24] Z. F. Chen, Q. P. Qin, J. L. Qin, J. Zhou, Y. L. Li, N. Li, Y. C. Liu, H. Liang, *J. Med. Chem.* **2015**, *58*, 4771.

[25] Q. Wu, K. D. Zheng, S. Liao, Y. Ding, Y. Q. Li, W. J. Mei, *Organometallics* **2016**, *35*, 317.

[26] C. M. Franz, G. E. Jones, A. J. Ridley, *Dev. Cell* **2002**, *2*, 153.

[27] M. Li, S. S. Ng, J. Wang, L. Lai, S. Y. Leung, M. Franco, Y. Peng, M. L. He, H. F. Kung, M. C. Lin, *Cancer Res.* **2006**, *66*, 1583.

[28] P. Friedl, K. Wolf, *Nat. Rev. Cancer* **2003**, *3*, 362.

[29] A. Bergamo, R. Gagliardi, V. Scarcia, A. Furlani, E. Alessio, G. Mestroni, G. Sava, *J. Pharmacol. Exp. Ther.* **1999**, *289*, 559.

[30] M. B. Kastan, J. Bartek, *Nature* **2004**, *432*, 316.

[31] M. V. Blagosklonny, *Aging (Albany NY)* **2011**, *3*, 94.

[32] J. Cao, Q. Wu, W. Zheng, L. Li, W. Mei, *RSC Adv.* **2017**, *7*, 26625.

[33] S. Zorzet, A. Bergamo, M. Cocchietto, A. Sorc, B. Gava, E. Alessio, E. Iengo, G. Sava, *J. Pharmacol. Exp. Ther.* **2000**, *295*, 927.

[34] E. Meulmeester, A. G. Jochemsen, *Curr. Cancer Drug Targets* **2008**, *8*, 87.

[35] B. Vogelstein, D. Lane, A. J. Levine, *Nature* **2000**, *408*, 307.

[36] J. Boyer, E. G. McLean, S. Aroori, P. Wilson, A. Mcculla, P. D. Carey, D. B. Longley, P. G. Johnston, *Clin. Cancer Res.* **2004**, *10*, 2158.

[37] C. Brantley-Finley, C. S. Lyle, L. Du, M. E. Goodwin, T. Hall, D. Szwedo, G. P. Kaushal, T. C. Chambers, *Biochem. Pharmacol.* **2003**, *66*, 459.

[38] Z. H. Siddik, *Oncogene* **2003**, *22*, 7265.

[39] M. J. Chow, C. Licona, D. Yuan Qiang, G. P. Wong, C. Gaiddon, W. H. Ang, *J. Med. Chem.* **2014**, *57*, 6043.

[40] I. Romero-Canelon, L. Salassa, P. J. Sadler, *J. Med. Chem.* **2013**, *56*, 1291.

[41] S. Chatterjee, S. Kundu, A. Bhattacharyya, C. G. Hartinger, P. J. Dyson, *J. Biol. Inorg. Chem.* **2008**, *13*, 1149.

[42] R. L. Hayward, Q. C. Schornagel, R. Tente, J. S. Macopherson, R. E. Aird, S. Guichard, A. Habtemariam, P. Sadler, D. I. Jodrell, *Cancer Chemother. Pharmacol.* **2005**, *55*, 577.

[43] M. A. Bennett, A. K. Smith, *Dalton Trans.* **1974**, 233.

[44] F. Mjambili, M. Njoroge, K. Naran, C. D. Kock, P. J. Smith, V. Mizrahi, D. Warner, K. Chibale, *Bioorg. Med. Chem. Lett.* **2014**, *24*, 560.

[45] G. Mestroni, E. Alessio, G. Sava, PCT. C07F 15/00, A61K 31/28, WO 98/00431 08.01.98, **1998**.

[46] C. M. Schempp, V. Kirkin, B. Simon-Haarhaus, A. Kersten, J. Kiss, C. C. Termeer, B. Gilb, T. Kaufmann, C. Borner, P. J. Sleeman, J. C. Simon, *Oncogene* **2002**, *21*, 1242.

How to cite this article: Wang L, He Y, Xiang G, Shang X. Synthesis, cytotoxicity and anti-metastatic properties of new pyridyl–thiazole arene ruthenium(II) complexes. *Appl Organometal Chem*. 2018;e4311. https://doi.org/10.1002/aoc.4311